scientific reports

Check for updates

OPEN

SDF-1α loaded lipid liquid crystalline hydrogel accelerates diabetic wound healing in in vitro and in vivo models

Farzad Sadri[1], Zohreh Rezaei[1,2], Hossein Safarpour[3], Hossein Kamali[4,5], Mehri Shadi[6], Pouria Mohammadparast-Tabas[7,8] & Mohammad Fereidouni[3]✉

Diabetes mellitus (DM) significantly impairs wound healing, often leading to chronic wounds with limited effective treatment options. Existing treatments often fail to provide sustained therapeutic effects, underscoring the need for advanced biomaterial-based approaches to enhance tissue regeneration. This study aimed to evaluate the wound healing efficacy of stromal cell-derived factor-1 alpha (SDF-1α)-loaded lipid liquid crystalline (LLC) hydrogel in both in vitro and in vivo models. A scratch wound healing assay was conducted on human dermal fibroblast (HDF) cells treated with allantoin (100 µg), LLC hydrogel, SDF-1α 50 ng/LLC, SDF-1α 25 ng/LLC, SDF-1α 25 ng, and a negative control. In vivo studies utilized diabetic rats ($n = 10$ per group) with full-thickness wounds, treated with LLC hydrogel, SDF-1α 300 ng/LLC, and polyhexamethylene biguanide (PHMB), compared to a negative control. Wound closure rates were measured on days 3, 7, 14, and 21, and histopathological analysis was performed. The SDF-1α/LLC hydrogel significantly enhanced HDF cell migration, showing a 32.8% improvement over the control ($P < 0.001$). Diabetic wounds treated with SDF-1α/LLC hydrogel demonstrated 51.4% faster closure by day 14 compared to the control ($P < 0.001$), with complete closure achieved by day 21. By day 21, SDF-1α/LLC and LLC hydrogels achieved 100% wound closure, while PHMB-treated wounds also exhibited significant healing, reaching 97.86% closure. Histological analysis revealed increased fibroblast proliferation, reduced inflammation, enhanced collagen deposition, and greater epithelial thickness, particularly in the SDF-1α/LLC group. The SDF-1α-loaded LLC hydrogel significantly enhances fibroblast migration, accelerates wound closure, and promotes tissue regeneration, making it a promising candidate for diabetic wound care.

Keywords SDF-1α, Lipid liquid crystalline hydrogel, Diabetic wound healing, Fibroblast migration, Tissue regeneration, STZ-diabetic model

Diabetes mellitus is a growing global health concern, with approximately 537 million adults currently affected—a number expected to reach 643 million by 2030 and 783 million by 2045[1].

One of the major complications associated with diabetes is impaired wound healing, often due to chronic inflammation and dysfunctional cellular responses[2]. These include insufficient recruitment of stem and progenitor cells, leading to delayed healing and increased risk of amputation, reduced quality of life, and higher mortality rates[3,4]. Effective wound healing necessitates the reestablishment of the skin's barrier through orchestrated processes such as cell mobilization, chemotaxis, and differentiation of bone marrow mesenchymal stem cells (BMSCs) and endothelial progenitor cells (EPCs)[5,6].

Stromal cell-derived factor-1 (SDF-1) is a key chemokine in this context, regulating the homing and migration of BMSCs, EPCs, and fibroblasts via interaction with the CXCR4 receptor, which is widely expressed

[1]Geriatric Health Research Center, Birjand University of Medical Sciences, Birjand, Iran. [2]Department of Biology, University of Sistan and Baluchestan, Zahedan, Iran. [3]Cellular and Molecular Research Center, Birjand University of Medical Sciences, Birjand, Iran. [4]Department of Pharmaceutics, School of Pharmacy, Mashhad University of Medical Sciences, Mashhad, Iran. [5]Targeted Drug Delivery Research Center, Pharmaceutical Technology Institute, Mashhad University of Medical Sciences, Mashhad, Iran. [6]Department of Anatomy, Faculty of Medicine, Birjand University of Medical Sciences, Birjand, Iran. [7]Student Research Committee, Birjand University of Medical Sciences, Birjand, Iran. [8]Department of Medical Biotechnology, Faculty of Medicine, Birjand University of Medical Sciences, Birjand, Iran. ✉email: dr.m.fereidouni@gmail.com

on hematopoietic and stromal cells[7–9]. This SDF-1/CXCR4 axis plays a central role in directing these cells to injury sites, particularly in diabetic wounds where cell recruitment is often impaired[10].

SDF-1α, the predominant isoform of SDF-1, has demonstrated superior biological activity in wound healing. It enhances the recruitment of progenitor cells, stimulates angiogenesis, and promotes fibroblast and keratinocyte proliferation[11]. However, in diabetic foot ulcers, endogenous levels of SDF-1α are often insufficient, contributing to reduced vascularization and poor tissue regeneration[12]. Maintaining an adequate and sustained concentration of SDF-1α at the wound site is essential, yet direct application is limited by enzymatic degradation, particularly by matrix metalloproteinases (MMPs), and poor tissue retention[13,14].

Despite promising preclinical data, clinical translation of SDF-1α-based therapies has been hampered by the lack of effective delivery systems. Most existing platforms fail to protect the protein or ensure its prolonged release. Biomaterials designed to overcome these limitations have shown potential, but none have fully addressed the stability and bioavailability challenges of SDF-1α in chronic wounds[15–17]. Recent studies underscore the therapeutic potential of controlled-release systems for enhancing SDF-1α efficacy. For instance, direct SDF-1α injection has been shown to reduce wound size in diabetic models, supporting the need for sustained delivery strategies[18,19].

Lipid liquid crystalline hydrogels present a promising solution due to their nanostructured matrices, biocompatibility, and capacity for encapsulating bioactive agents[20,21]. These properties enable them to protect sensitive molecules from degradation and provide extended release, making them suitable for chronic wound environments.

While LLC systems have been widely explored for other biomolecules, their application in delivering SDF-1α for diabetic wound healing remains uninvestigated. Given their ability to maintain local therapeutic concentrations and support tissue regeneration[22]we propose the development of an SDF-1α-loaded LLC hydrogel as a novel strategy for diabetic wound repair.

This study aims to evaluate whether such a hydrogel can enhance healing by promoting fibroblast migration, angiogenesis, and tissue regeneration. We hypothesize that this system will provide sustained release of SDF-1α and improve wound healing outcomes compared to conventional approaches, using both in vitro and in vivo models.

Results

Dynamic light scattering analysis

Dynamic light scattering analysis revealed a mean effective particle diameter of 133.80 ± 6.26 nm, with a polydispersity index (PDI) of 0.216 ± 0.038, indicating variability across replicates. The baseline index averaged 6.2 ± 4.4, confirming stable measurement conditions. The count rate was 95.5 ± 4.3 kcps with 100% data retention, ensuring measurement reliability.

The mean diameters by intensity, number, and volume were 160.92 ± 19.98 nm, 44.55 ± 13.89 nm, and 67.25 ± 8.71 nm, respectively, indicating a polydisperse particle size distribution (Fig. 1A, B and C). The diffusion coefficient was $3.673 \times 10^{-8} \pm 1.709 \times 10^{-9}$ cm^2/s, falling within expected theoretical ranges for nanoparticles of this size. The reported values characterize the size distribution and stability of the nanoparticles in solution.

Hexosome phases in hydrogel

The PLM confirmed the presence of hexosome phases within the LLC hydrogel, identified by their bright and elongated birefringence patterns. These birefringence patterns are indicative of hexosome organization. While hexosome phases were predominant, cubosome structures were also detected, characterized by their low birefringence and dark appearance under polarized light microscopy (Fig. 1D, E).

Rheological characterization

The rheological behavior of LLC hydrogel formulations was analyzed using the Brookfield R/S PLUS rheometer to evaluate viscosity and shear stress responses. The LLC hydrogel exhibited Newtonian fluid behavior at low shear rates, transitioning to a shear-thinning, non-Newtonian behavior as shear stress increased from 0 to 100 Pa. At 25 °C, viscosity initially measured approximately 1200 cP at zero shear stress, gradually decreasing to 200 cP at 100 Pa shear stress. The viscosity profile shows a reduction with increasing shear, indicating shear-thinning behavior. Detailed viscosity data are presented in Table S1.

Water uptake/loss

The water uptake and retention properties of the LLC precursor were assessed using Karl Fischer titration following a 7-day immersion in PBS under controlled conditions. The hydrogel absorbed 33.2 ± 2.3% of its weight in water after 168 h, while minimal water loss was observed upon drying. The hydrogel exhibited a high-water retention capacity after immersion.

Degradation analysis of the LLC hydrogel formulation

The mass loss of the LLC hydrogel formulation was monitored over 60 days (Fig. 2A). A rapid initial degradation phase occurred within the first 14 days, followed by a gradual decline.

Degradation percentages at days 1, 4, 7, 14, 21, 28, 42, and 60 were recorded (Fig. 2B). The hydrogel exhibited 7% degradation by day 4, 25% by day 14, 40% by day 28, and 71% by day 60. The degradation profile demonstrates a progressive reduction in hydrogel mass over the study period.

In vitro release profile

The release kinetics of SDF-1α from a 100 µL LLC hydrogel loaded with 2000 ng was studied over 144 h (Fig. 2C). An initial burst release phase occurred, with 9.16% of SDF-1α released at zero-hour, followed by 25.21% at 1 h

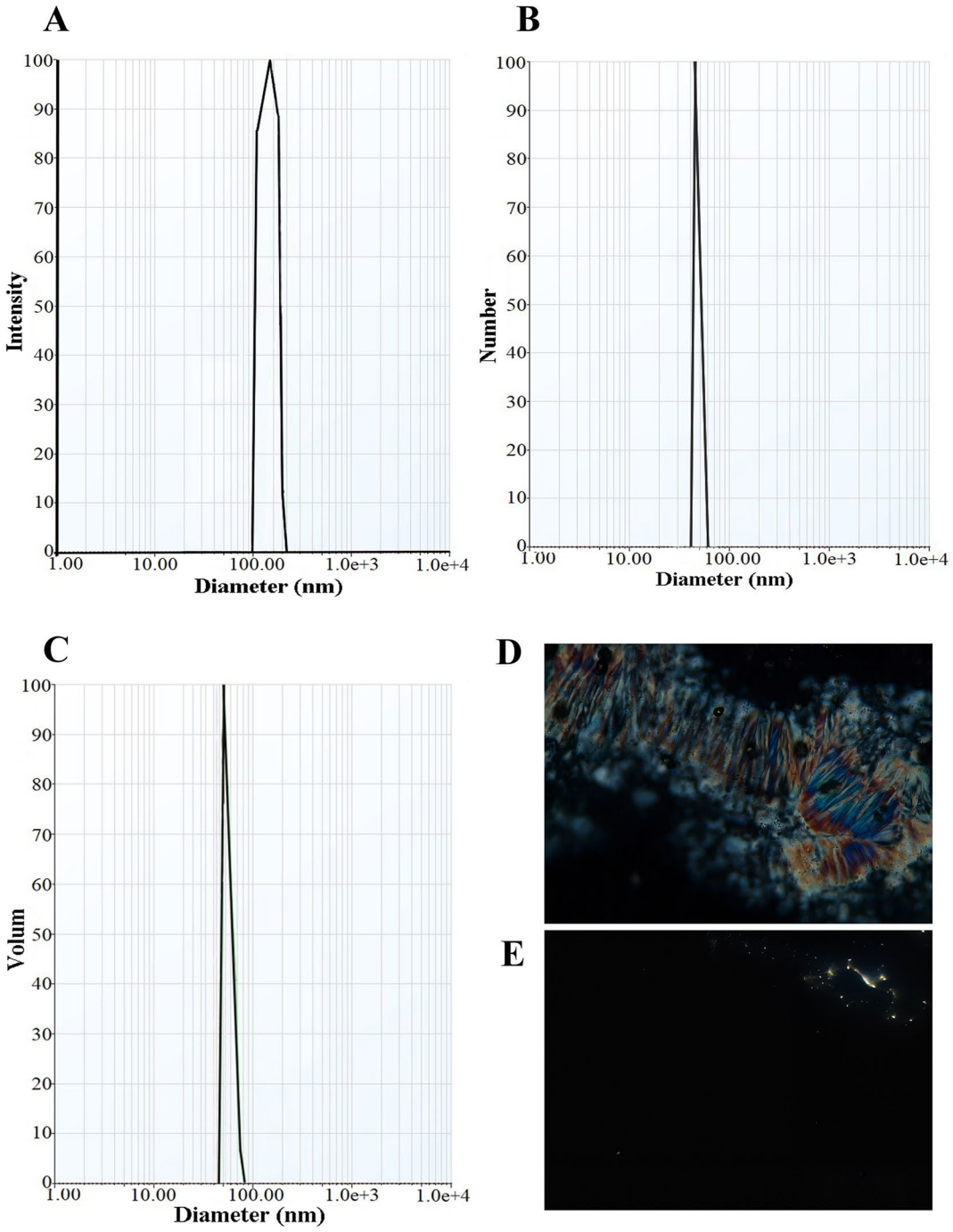

Fig. 1. Characterization of formulations through dynamic light scattering and polarized light microscopy. (**A**) Number distribution of particles by diameter (nm), (**B**) Intensity distribution of particles by diameter (nm), and (**C**) Volume distribution of particles by diameter (nm). (**D**) Hexosome exhibiting hexagonal patterns due to the birefringence of the hexagonal (HII) phase, and (**E**) Cubosome characterized by dark regions indicating minimal birefringence associated with the cubic phase.

and 37.32% at 2 h. The release rate then slowed, reaching 43.03% by 4 h and 46.91% by 6 h. By 24 h, 73.31% of the total SDF-1α had been released, followed by 84.97% at 48 h and 90.71% at 72 h. By the end of the observation period (144 h), cumulative release reached 94.69%. The cumulative release profile indicates an initial burst phase followed by sustained release over time.

Cell viability results

Treatment of human dermal fibroblasts with various concentrations of SDF-1 and LLC revealed a significant reduction in cell viability only at the highest SDF-1 concentration (800 ng/mL), where the mean cell viability

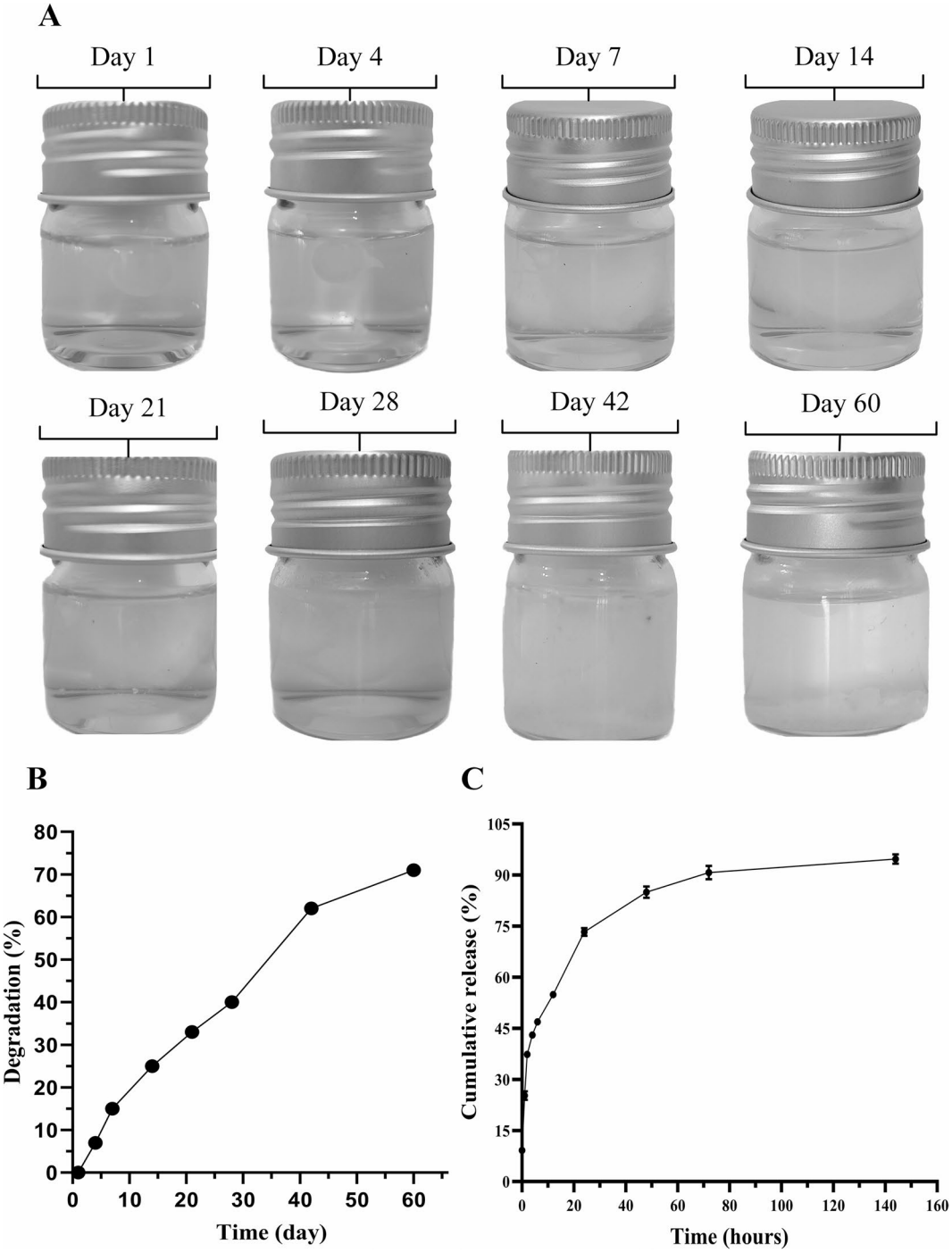

Fig. 2. Degradation and release dynamics of LLC hydrogel. (**A**) Sequential images of vials containing the LLC hydrogel formulation on days 1, 4, 7, 14, 21, 28, 42, and 60, visually demonstrating the gradual degradation and structural changes of the hydrogel matrix over time. (**B**) A degradation curve showing the percentage of hydrogel degradation at each of these time points, clearly illustrating the reduction in structural integrity over the 60-day period. (**C**) Release profile of SDF-1α from the LLC hydrogel over specific time intervals (1, 2, 4, 6, 24, 48, 72, and 144 h), demonstrating a sustained and controlled release pattern essential for the effective delivery of the bioactive compound.

decreased to 90.1% compared to the control ($p = 0.046$) (Fig. 3C). At all other SDF-1 concentrations (400–6.25 ng/mL) and across all tested LLC doses, cell viability remained comparable to the control group, consistently exceeding 95% and showing no statistically significant differences. These findings indicate that SDF-1 exerts a dose-dependent cytotoxic effect only at supraphysiological concentrations, whereas lower concentrations of SDF-1 and all tested doses of LLC are well tolerated by human dermal fibroblasts under these experimental conditions.

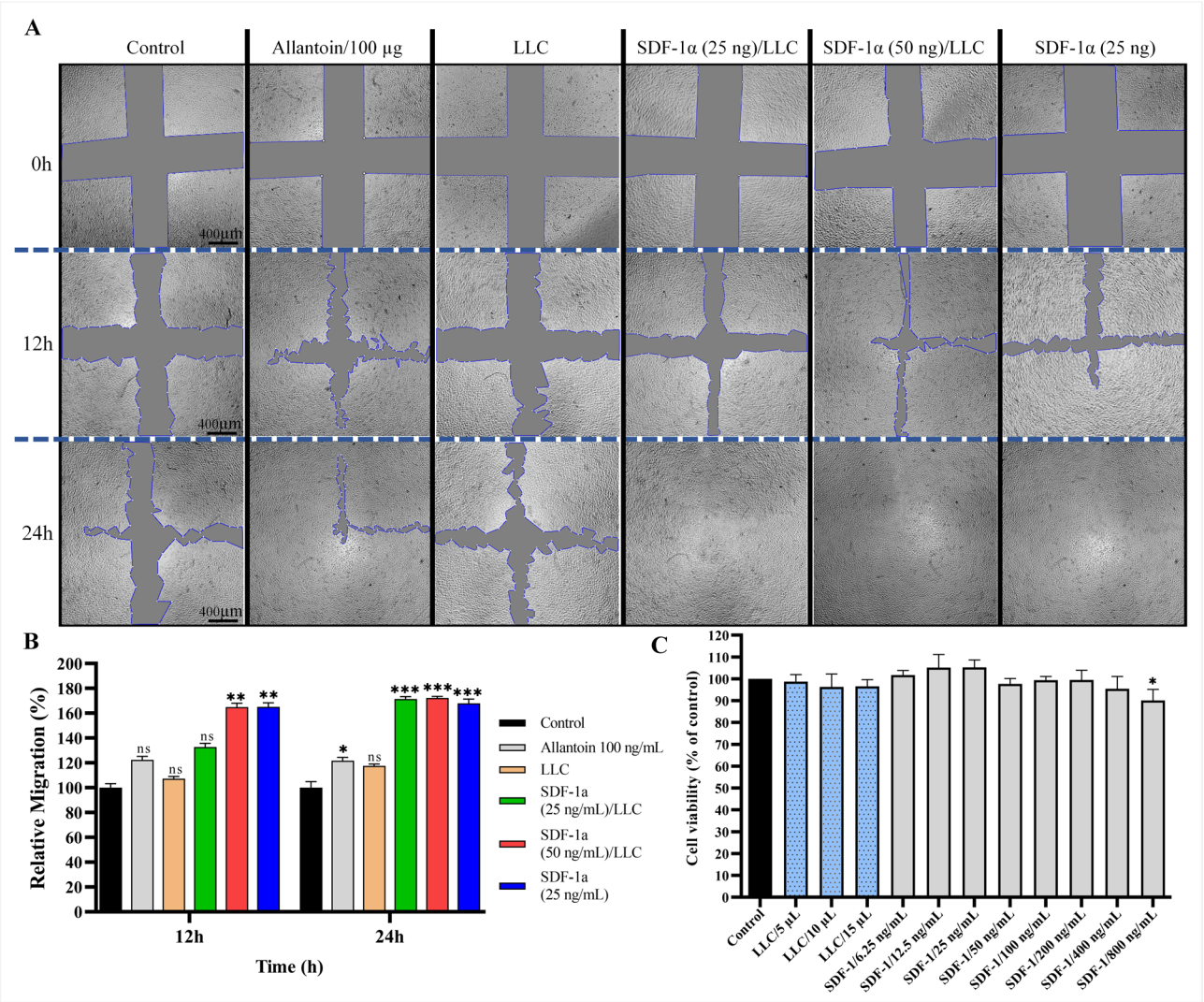

Fig. 3. Relative migration percentage in scratch wound healing assay. (**A**) A series of images depicting the wound healing process at 0, 12, and 24 h for HDF cells treated with various formulations, including allantoin 100 µg, LLC, SDF-1α 50 ng/LLC, SDF-1α 25 ng/LLC, SDF-1α 25 ng, and a negative control (4× magnification; scale bar = 400 µm. (**B**) A chart illustrating relative migration percentage at 0, 12, and 24 h for the different treatment groups. (**C**) Cell viability of human dermal fibroblasts following 24 h exposure to varying concentrations of SDF-1 (6.25–800 ng/mL) and LLC (5, 10, 15 µL), assessed by MTT assay. Data are mean ± SD ($n = 4$). Statistical analysis was performed using one-way ANOVA followed by Tukey's post hoc test, with significance levels are marked as $^{*}P < 0.05$, $^{**}P < 0.01$, $^{***}P < 0.001$, ns for non-significant differences, compared to the negative control.

Scratch wound healing assay

A scratch wound healing assay was conducted using HDF cells to evaluate cell migration and wound closure over 24 h (Fig. 3A). At 12 h, treatments with SDF-1α at 25 ng/mL and 50 ng/mL/LLC significantly improved wound closure compared to the control group ($P < 0.01$) and the LLC-only group ($P < 0.05$). At 24 h, SDF-1α/LLC at 25 ng/mL and 50 ng/mL, as well as SDF-1α at 25 ng/mL alone, significantly enhanced wound closure compared to the control ($P < 0.001$). The allantoin-treated group exhibited statistically significant wound closure compared to the control ($P < 0.05$) (Fig. 3B).

In vivo study on diabetic wound healing

This study evaluated the effectiveness of LLC hydrogel, PHMB, and SDF-1α/LLC hydrogel in promoting wound healing in diabetic rats by monitoring wound closure rates over a 21-day period (Fig. 4A). On day 3, statistical analysis revealed significant differences in wound closure rates among the groups. The control group showed 39.47% closure, while LLC hydrogel, PHMB, and SDF-1α/LLC hydrogel groups showed 55.11% ($P < 0.05$), 51.38%, and 67.41% ($P < 0.01$), respectively. A significant improvement in wound closure was observed in the treatment groups by day 3, indicating an early therapeutic effect. On day 3, no significant differences were

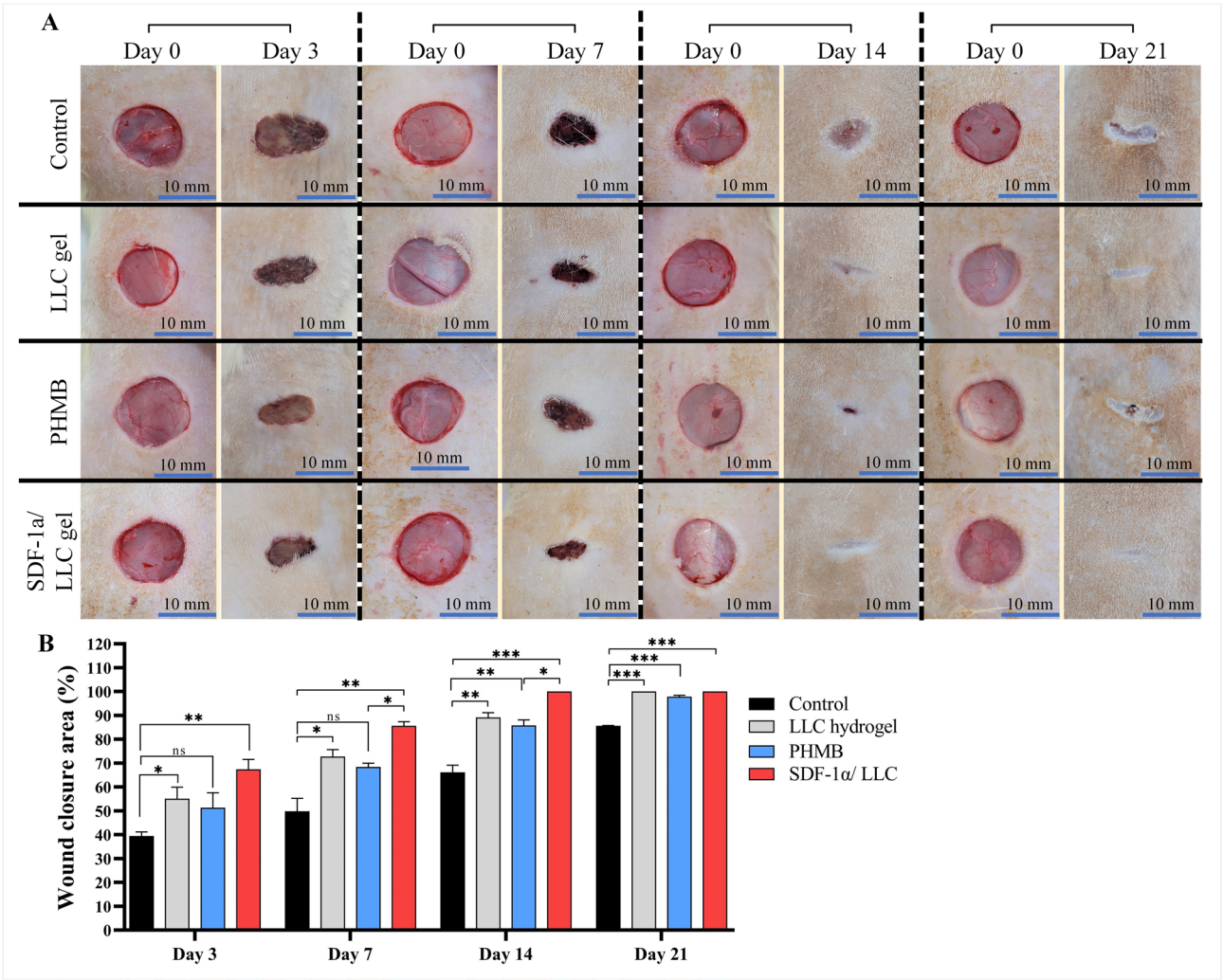

Fig. 4. Wound closure was significantly enhanced in SDF-1α/LLC hydrogel -treated wounds compared to the control. (**A**) Photos of wounds treated with LLC hydrogel, PHMB, SDF-1α/LLC hydrogel, and control (normal saline). Images are shown with a scale bar of 10 mm. (**B**) Chart shows percentage wound closure areas at days 3, 7, 14, and 21 for control, LLC hydrogel, PHMB and SDF-1α/LLC hydrogel; each animal received a one treatment type across all wounds. Statistical analysis was performed using one-way ANOVA followed by Tukey's post hoc test, with significance levels indicated as $^{*}P<0.05$, $^{**}P<0.01$, $^{***}P<0.001$, and ns for non-significant differences, compared to control, $n=10$.

observed among the treatment groups (LLC hydrogel, PHMB, SDF-1α/LLC), although all were significantly better than control.

On day 7, the differences became more pronounced, particularly in the SDF-1α/LLC hydrogel group, which showed 85.68% wound closure, significantly higher than the control group's 49.85% ($P<0.01$). The LLC hydrogel and PHMB treatments also showed improvements, with wound closures of 72.80% ($P<0.05$) and 68.38%, respectively. These findings demonstrate differential wound healing rates among the treatment groups. On day 7, SDF-1α/LLC hydrogel showed significantly higher wound closure than PHMB ($P<0.05$), while no other differences among treatment groups reached significance.

By day 14, results indicated that SDF-1α/LLC hydrogel achieved 100% wound closure, significantly outperforming the control group at 66.11% ($P<0.001$). The LLC hydrogel and PHMB treatments also showed substantial healing rates of 89.15% and 85.81%, respectively ($P<0.01$). The observed wound closure rates highlight the sustained effectiveness of the hydrogel-based treatments. On day 14, SDF-1α/LLC hydrogel had significantly higher wound closure compared to PHMB ($P<0.05$); other treatment groups were not significantly different from each other. On day 21, the final observations showed that all treatment groups had significantly better outcomes compared to the control ($P<0.001$). The LLC hydrogel and SDF-1α/LLC hydrogel groups achieved complete wound closure (100%), while PHMB-treated wounds closed by 97.86%. By day 21, there were no significant differences in wound closure rates among the treatment groups (Fig. 4B).

Histopathological analysis

Fibroblast proliferation and inflammatory cell infiltration

This study evaluated fibroblast proliferation and inflammatory cell infiltration across three treatment groups (LLC, PHMB, and SDF-1α/LLC) and a control group at intervals of 3, 7, 14, and 21 days. The results indicated progressive changes in cell populations during wound healing (Fig. 5A).

On day 3, the SDF-1α/LLC group exhibited a significantly higher mean fibroblast count (218.4 ± 12.09 cells/field) compared to the control group (154.2 ± 8.99 cells/field). The fibroblast counts in the LLC hydrogel (198.2 ± 14.63 cells/field) and PHMB (169.8 ± 4.04 cells/field) groups did not significantly differ from the control. On day 7, the SDF-1α/LLC group maintained a significantly higher mean fibroblast count (377 ± 24.6 cells/field) compared to the control group (270.4 ± 16.68 cells/field). The LLC hydrogel (323.2 ± 28.89 cells/field) and PHMB (334.8 ± 14.66 cells/field) groups exhibited increases in fibroblast count, though these differences were not statistically significant.

On day 14, fibroblast counts remained comparable between the control group (214.2 ± 9.6 cells/field) and the treatment groups: LLC (210.6 ± 21.44 cells/field), PHMB (208.8 ± 7.05 cells/field), and SDF-1α/LLC (232.8 ± 16.15 cells/field). On day 21, the SDF-1α/LLC group demonstrated a significantly higher mean fibroblast count (213.8 ± 19.22 cells/field) compared to the control group (165 ± 5.32 cells/field). The LLC hydrogel (202.8 ± 3.97 cells/field) and PHMB (180 ± 3.08 cells/field) groups did not show statistically significant differences relative to the control group (Fig. 5B).

The extent of inflammatory cell infiltration was significantly lower in the treatment groups compared to the control group, with the LLC hydrogel and SDF-1α/LLC groups showing the most notable reductions. On day 3, the LLC hydrogel group had a significantly lower mean inflammatory cell count (90.6 ± 5.43 cells/

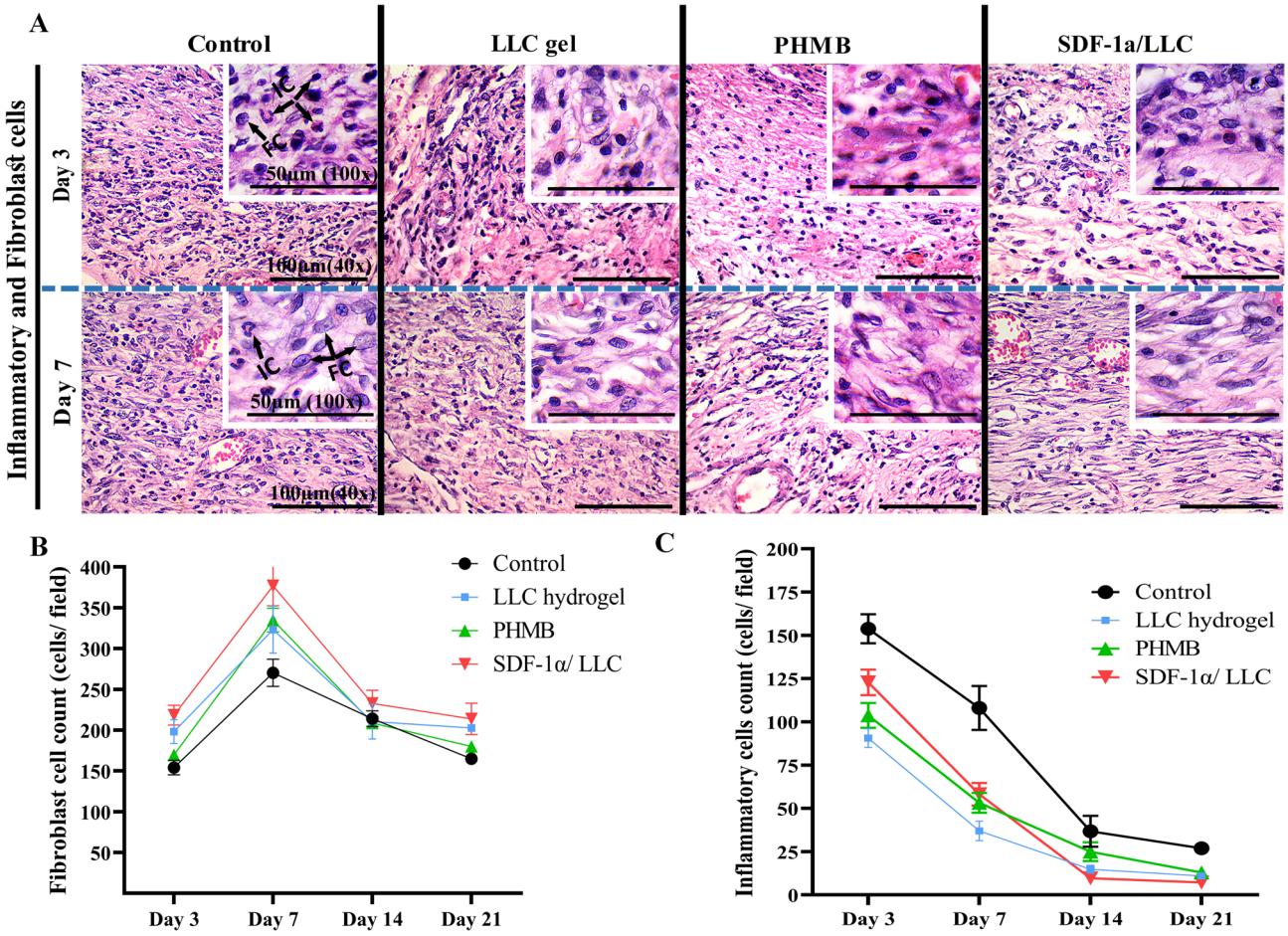

Fig. 5. Cellular responses during wound healing across different treatment groups. (**A**) Representative images of fibroblast cells and Inflammatory cell infiltration in wound tissue sections from LLC hydrogel, SDF-1α/LLC, and PHMB, and control groups at days 3 and 7 post-injuries. Black arrows labeled IC and FC indicate inflammatory cells and fibroblast cells, respectively (H&E stain; 40× magnification; scale bar = 100 µm). All images are transverse sections. (**B**) Quantification of inflammatory cell count (cells/field) from ten random fields per sample. (**C**) Quantification of fibroblast cell count (cells/field) from ten random fields per sample. Data are shown as mean ± SEM ($n = 5$ per group). Statistical analysis was conducted using one-way ANOVA followed by Tukey's post hoc test (*$P < 0.05$, **$P < 0.01$, ***$P < 0.001$, and ns = non-significant, compared to control group).

field) compared to the control group (153.8 ± 8.45 cells/field). The PHMB group also showed a significant reduction (103.8 ± 7.27 cells/field), while the reduction in the SDF-1α/LLC group (122.8 ± 7.42 cells/field) was not statistically significant. On day 7, significant reductions in inflammatory cell infiltration were observed in the LLC hydrogel (37 ± 5.69 cells/field), PHMB (53.2 ± 5.71 cells/field), and SDF-1α/LLC (58.2 ± 6.48 cells/field) groups compared to the control group (108 ± 12.71 cells/field).

On day 14, inflammatory cell infiltration was significantly reduced in the LLC hydrogel (14.8 ± 2.35 cells/field) and SDF-1α/LLC (9.6 ± 2.38 cells/field) groups compared to the control group (36.8 ± 8.92 cells/field). Although the PHMB group (25 ± 5.4 cells/field) exhibited a decrease, this reduction was not statistically significant. On day 21, all treatment groups exhibited highly significant reductions in inflammatory cell infiltration compared to the control group (27 ± 2.3 cells/field): LLC hydrogel (11 ± 1.45 cells/field), PHMB (13 ± 1.7 cells/field), and SDF-1α/LLC (7.2 ± 1.59 cells/field). (Fig. 5C).

Angiogenesis

The angiogenesis evaluation following wound treatment revealed significant differences among the treatment groups (Fig. 6A).

On day 3, the LLC hydrogel (4.8 ± 0.49 vessels/field) and SDF-1α/LLC (5.4 ± 0.68 vessels/field) groups exhibited significantly higher vessel formation compared to the control group (2 ± 0.37 vessels/field) ($P < 0.01$). Both the SDF-1α/LLC and LLC hydrogel groups demonstrated significantly enhanced angiogenesis relative to the control group. On day 7, the LLC hydrogel (5.75 ± 0.57 vessels/field), PHMB (6 ± 0.63 vessels/field), and SDF-1α/LLC (8.33 ± 0.76 vessels/field) groups showed significantly higher vessel formation compared to the control group (3.33 ± 0.33 vessels/field) ($P < 0.001$). Comparisons indicated significant differences between the control

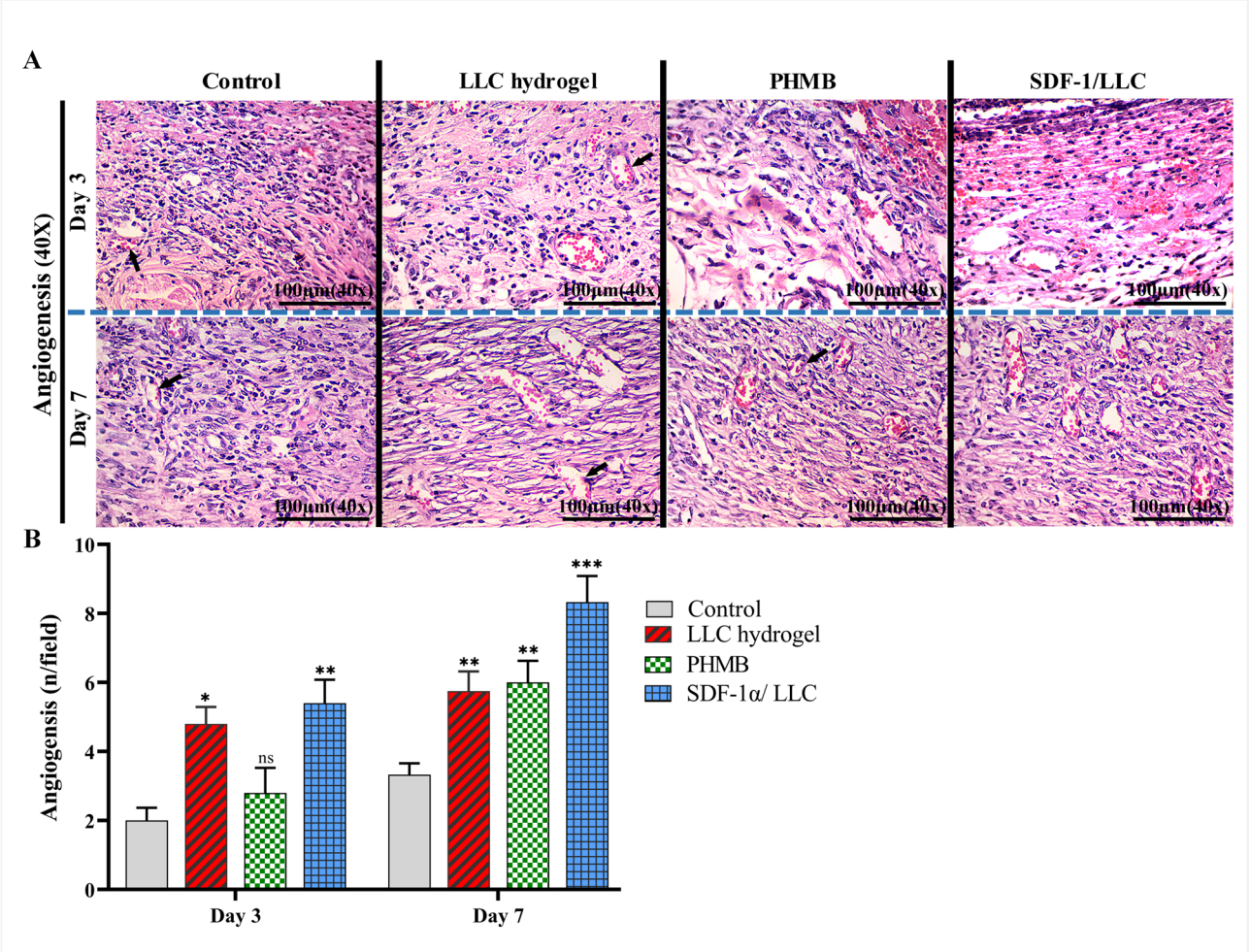

Fig. 6. Angiogenesis in wound healing at early stages across treatment groups. (**A**) Representative images of newly formed blood vessels (marked by black arrows) in wound tissue sections from LLC hydrogel, SDF-1α/LLC, and PHMB, and control groups at days 3 and 7 post-injury (H&E stain; 40× magnification; scale bar = 100 μm). All images are transverse sections. (**B**) Quantification of angiogenesis (vessels/field) from ten random fields per sample. Data are shown as mean ± SEM ($n = 5$ per group). Statistical analysis was conducted using one-way ANOVA followed by Tukey's post hoc test (*$P < 0.05$, **$P < 0.01$, ***$P < 0.001$, and ns = non-significant).

and LLC hydrogel groups ($P < 0.05$), the control and PHMB groups ($P < 0.01$), and the control and SDF-1α/LLC groups ($P < 0.001$) (Fig. 6B).

Collagen synthesis

The evaluation of collagen synthesis following treatment revealed significant differences among the treatment groups (Fig. 7A).

On day 14, the SDF-1α/LLC group exhibited significantly higher collagen deposition (0.165 ± 0.006 µm) compared to the control group (0.084 ± 0.007 µm) ($P < 0.01$). Increased collagen deposition was also observed in the LLC hydrogel (0.107 ± 0.010 µm) and PHMB (0.103 ± 0.004 µm) groups.

On day 21, the LLC hydrogel (0.258 ± 0.011 µm) and SDF-1α/LLC (0.308 ± 0.006 µm) groups exhibited significantly higher collagen deposition compared to the control group (0.231 ± 0.011 µm) ($P < 0.001$). The PHMB group exhibited an increase in collagen deposition (0.244 ± 0.010 µm), though this was moderate compared to the other treatment groups (Fig. 7B).

Enhanced epithelialization microscopic observations

By day 14 post-wounding, the wound area in the treatment groups was visibly smaller compared to the control group. By day 21, the treatment groups exhibited further wound closure, with the SDF-1α/LLC and LLC hydrogel groups displaying complete re-epithelialization and well-organized collagen fibers.

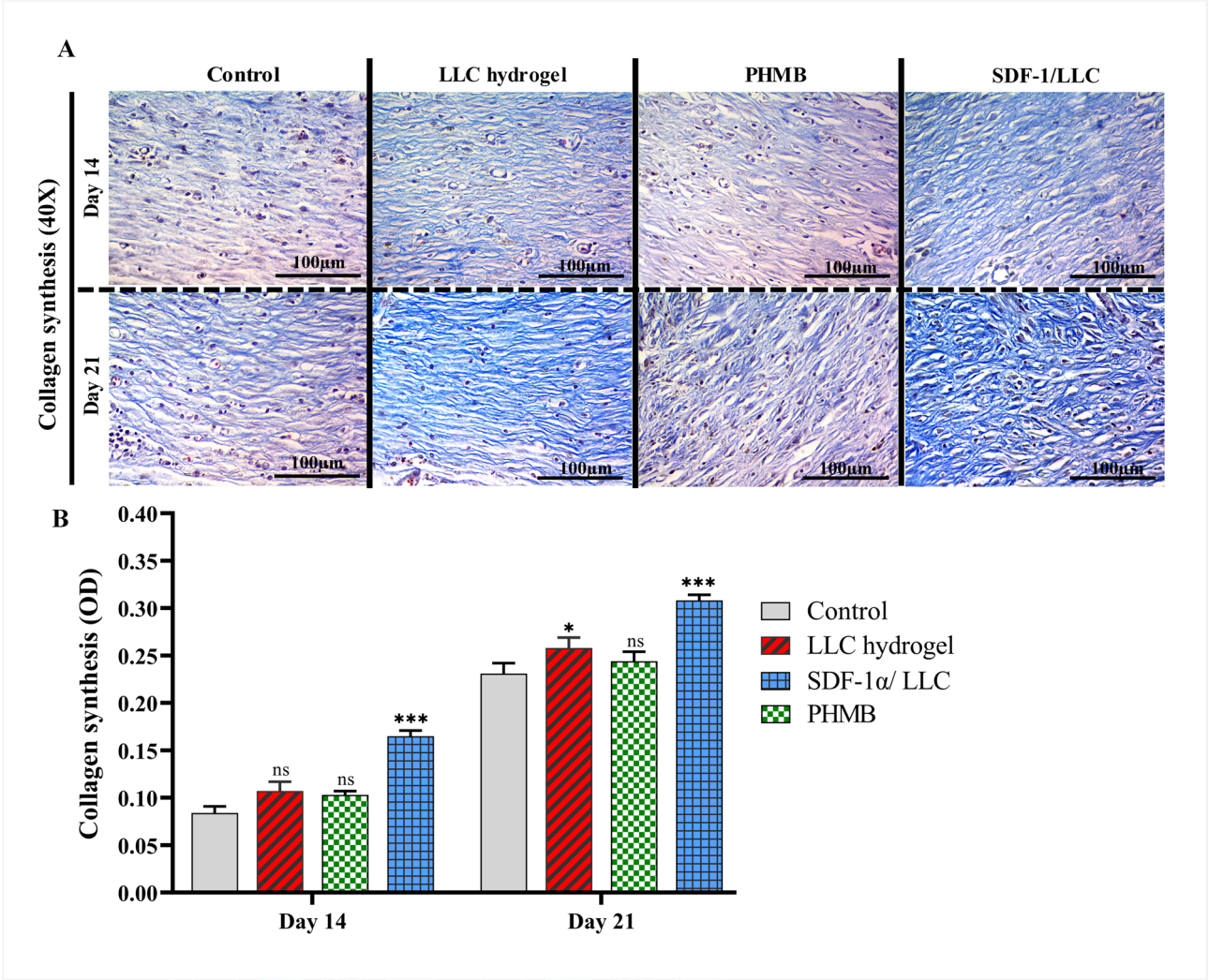

Fig. 7. Collagen synthesis during wound healing in different treatment groups. (**A**) Representative images of collagen fibers in wound tissue sections from LLC hydrogel, SDF-1α/LLC, and PHMB, and control groups at days 14 and 21 post-injury (Masson's trichrome stain; 40× magnification; scale bar = 100 µm). Images were captured at 40× magnification. All images are transverse sections. (**B**) Quantification of collagen synthesis (µm) from ten random fields per sample. Data are shown as mean ± SEM ($n = 5$ per group). Statistical analysis was conducted using one-way ANOVA followed by Tukey's post hoc test (*$P < 0.05$, **$P < 0.01$, ***$P < 0.001$, and ns = non-significant, compared to control).

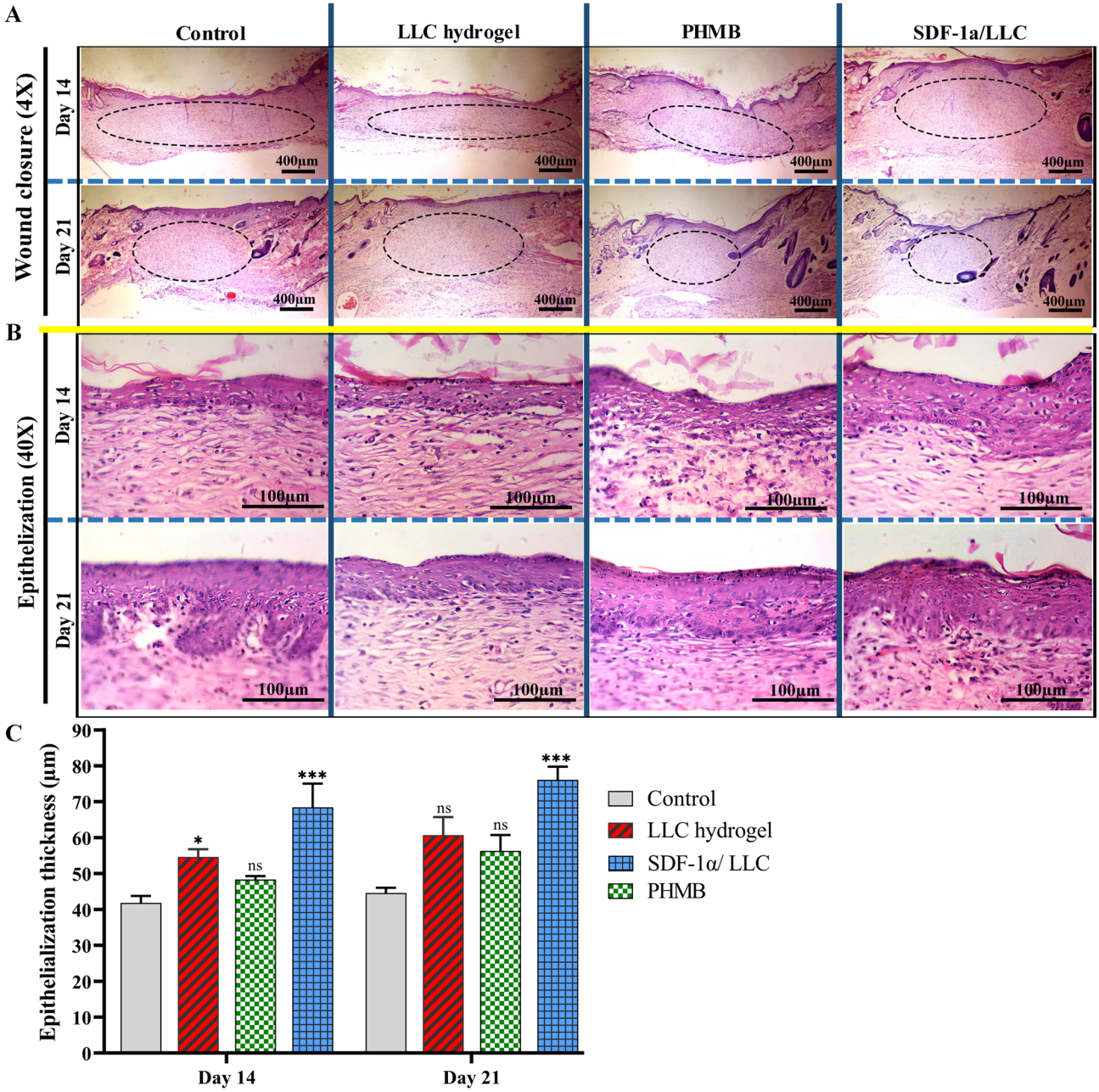

Fig. 8. Wound closure area and epithelialization during wound healing in different treatment groups. (**A**) Representative images of wound tissue sections from LLC hydrogel, SDF-1α/LLC, and PHMB, and control groups at days 14 and 21 post-injury. The wound closure area is highlighted with an elliptical dashed line (H&E stain; 4× magnification; scale bar = 400 μm). (**B**) Representative images showing epithelial thickness in the wound tissue sections from the same groups at days 14 and 21 post-injury (H&E stain; 40× magnification; scale bar = 100 μm). Images were captured at 40× magnification. (**C**) Quantification of epithelial thickness (μm) and wound closure area (%) from ten random fields per sample. Data are shown as mean ± SEM ($n = 5$ per group). Statistical analysis was conducted using one-way ANOVA followed by Tukey's post hoc test (*$P < 0.05$, **$P < 0.01$, ***$P < 0.001$, and ns = non-significant, compared to control).

The control group exhibited a larger wound area with persistent inflammatory signs and incomplete epithelial coverage (Fig. 8A). To evaluate the effectiveness of different treatments, epithelial thickness in wound areas was measured (Fig. 8B). On day 14, the SDF-1α/LLC group exhibited a mean epithelial thickness of 68.46 ± 6.6 μm, which was significantly greater ($P < 0.001$) than both the control group (41.83 ± 1.94 μm) and the PHMB group (48.32 ± 0.97 μm). A significant increase in epithelial thickness was also observed in the LLC hydrogel group (54.65 ± 2.15 μm). By day 21, the SDF-1α/LLC group maintained superior epithelialization, with a mean thickness of 76.07 ± 3.69 μm, significantly surpassing the control group's 44.58 ± 1.50 μm ($P < 0.001$).

The LLC hydrogel and PHMB groups also exhibited increased epithelial thicknesses of 60.67 ± 5.09 µm and 56.33 ± 4.41 µm, respectively (Fig. 8C).

Discussion

Diabetes significantly impairs wound healing due to dysfunctional fibroblasts, epidermal cells, failed angiogenesis, and impaired tissue maturation[23]. Additionally, diabetes leads to decreased wound contraction and re-epithelialization, increasing the risk of infection, repeated hospitalization, and amputation[24]. Consequently, there is an urgent need for innovative, safe, and effective wound healing strategies to reduce patient morbidity and the economic burden associated with this clinical challenge. Given the critical role of angiogenesis in wound healing, this study evaluated the effects of sustained SDF-1α release through LLC hydrogel on diabetic wound healing.

Dynamic Light Scattering Analysis revealed a mean particle diameter of 133.80 ± 3.61 nm, indicating a relatively uniform size distribution crucial for consistent drug delivery. The LLC hydrogel matrix provided a stable and controlled release of SDF-1α, ensuring its sustained availability at the wound site. The amphiphilic nature of LLC hydrogels, which allows them to encapsulate and gradually release bioactive molecules, offers an advantage over conventional delivery systems[25]. This sustained release is crucial, given the challenges of maintaining therapeutic concentrations of SDF-1α in the wound environment, and likely contributed to the observed improvements in wound healing in our study. Karimi et al. (2023) also demonstrated that LLC formulations enhance drug delivery efficiency by providing sustained release, improving local drug concentration, and reducing systemic side effects[26].

The Rheological Characterization of the LLC hydrogel showed that it transitions from Newtonian to shear-thinning behavior, facilitating easy application to wound sites while maintaining structural integrity. This property, combined with the hydrogel's ability to absorb and retain significant amounts of water (33.2 ± 2.3% after 168 h), supports a moist wound environment, crucial for tissue regeneration.

In the in vitro studies, the scratch wound healing assay demonstrated that SDF-1α significantly enhances cell migration. After 24 h of treatment, both SDF-1α-loaded LLC hydrogel and SDF-1α alone significantly increased cell migration ($P < 0.05$) compared to the control group. This observation is consistent with previous studies, such as Zhu et al. (2016), which reported that the continuous release of SDF-1 from antioxidant hydrogels significantly increased HUVEC migration[27]. The enhanced cell migration can be attributed to SDF-1α's chemotactic properties, which recruit essential cells like mesenchymal stem cells, endothelial progenitor cells, and fibroblasts to the wound site, critical in diabetic wounds where cell migration is often impaired[19,28,29].

The in vivo study using STZ-induced diabetic rat models showed that SDF-1α-loaded LLC hydrogel significantly improved wound closure rates over a 21-day period compared to control groups ($P < 0.05$). Histological analysis further supported these findings, showing enhanced fibroblast proliferation, reduced inflammatory cell infiltration, increased angiogenesis, collagen synthesis, and epithelialization in the SDF-1α/LLC-treated wounds compared to controls. These results align with the literature, where the use of SDF-1α has been shown to significantly enhance key aspects of the wound healing process. For instance, Zhu et al. (2016) observed similar improvements in fibroblast proliferation, reduction in inflammatory cells, increased angiogenesis, and collagen deposition when using SDF-1α-loaded hydrogels[27]. These enhancements are critical for the effective repair and regeneration of damaged tissues, particularly in diabetic wounds where healing is typically impaired. Similarly, Yao et al. (2020) demonstrated that SDF-1-loaded genipin-crosslinked chitosan scaffolds enhanced wound healing by promoting neovascularization and increasing VEGF expression. Their study found that diabetic wounds treated with SDF-1/GC scaffolds showed higher recovery rates compared to control treatments[29].

Furthermore, Li et al. (2016) demonstrated that SDF-1 promotes chronic wound healing by enhancing fibroblast proliferation, reducing inflammatory cell infiltration, increasing angiogenesis, and promoting collagen synthesis and epithelialization[30].

Rabbany et al. (2010) also demonstrated that continuous delivery of SDF-1 from alginate scaffolds significantly accelerates wound healing. Their study showed that SDF-1-treated wounds exhibited enhanced fibroblast infiltration, increased angiogenesis, and reduced scarring compared to controls. The SDF-1-treated wounds achieved significantly faster closure rates, with 38% of wounds fully healed by day 9 compared to none in the control group[31]. The enhanced wound healing observed can be attributed to several mechanisms facilitated by SDF-1α. SDF-1α is known for its chemotactic properties, recruiting cells to the wound site—a critical process in diabetic wounds where cell migration is often impaired. Moreover, SDF-1α promotes angiogenesis, essential for forming new blood vessels and subsequent tissue repair[10]. Our histological analyses supported these mechanisms, showing increased collagen deposition, reduced inflammation, and enhanced re-epithelialization in treated wounds.

The therapeutic effects observed in this study—including faster wound closure, enhanced fibroblast proliferation, angiogenesis, reduced inflammation, and increased collagen synthesis—are mainly mediated by SDF-1α through its receptor CXCR4. Activation of CXCR4 by SDF-1α triggers downstream signaling pathways such as PI3K/AKT, MAPK/ERK, and JAK/STAT, which are essential for promoting endothelial cell migration and angiogenesis, boosting fibroblast function and collagen deposition, and modulating immune responses to limit inflammation. These mechanisms are especially important in the diabetic wound microenvironment, where chronic inflammation, hypoxia, and impaired cell migration inhibit normal healing. Thus, CXCR4-mediated signaling by SDF-1α can help overcome these barriers and restore tissue repair, as observed in the SDF-1α/LLC hydrogel-treated group[10,27,32].

Compared to conventional hydrogel systems such as alginate, chitosan, or synthetic polymer hydrogels, LLC hydrogels offer several unique advantages for the delivery of SDF-1α. The unique structural characteristics of LLC hydrogels contribute significantly to these advantages. LLC hydrogels possess a self-assembled, ordered structure

with controlled porosity, allowing for sustained and regulated release of encapsulated bioactive molecules such as SDF-1α[33]. Furthermore, while alginate-based hydrogels provide controlled release, their delivery profiles can be significantly affected by external fluid flows, potentially leading to less predictable release kinetics[34]. Chitosan-based hydrogels, although biocompatible and bioresorbable, often require crosslinking and combination with other materials to enhance mechanical properties, and their release behavior can be difficult to precisely control without chemical modification[35]. Synthetic polymer hydrogels like OPF exhibit favorable mechanical properties but their porous structure can introduce variability in drug release profiles, particularly causing burst release at high therapeutic loadings[36]. Thus, LLC hydrogels naturally possess amphiphilic properties, enabling superior encapsulation efficiency, protecting sensitive biological molecules from rapid enzymatic degradation, and ensuring prolonged bioactivity of therapeutic agents like SDF-1α[33].

The promising results suggest that SDF-1α-loaded LLC hydrogel has significant potential as a therapeutic agent for diabetic wound healing. Future clinical trials are essential to confirm its efficacy and safety in human subjects. Additionally, optimizing SDF-1α concentration and release kinetics within the LLC hydrogel could further enhance its therapeutic potential. Developing such advanced wound dressings could substantially reduce the burden of chronic wounds in diabetic patients, improving their quality of life and reducing healthcare costs.

Despite these positive findings, the study has limitations. The use of animal models, while informative, may not fully replicate the complexities of human diabetic wound healing. Therefore, clinical trials are necessary to validate these results. Additionally, the potential cytotoxicity of high concentrations of SDF-1α observed in some in vitro assays highlights the need for careful dose optimization[37,38].

Conclusion

The SDF-1α-loaded LLC hydrogel demonstrated significant potential in enhancing wound healing in diabetic models by promoting cell migration and wound closure. This study underscores the importance of developing innovative delivery systems for bioactive molecules like SDF-1α, which can overcome the challenges of chronic wound healing in diabetic patients. The results also highlight the comprehensive benefits of SDF-1α/LLC treatment, including improvements in fibroblast proliferation, inflammatory cell reduction, angiogenesis, collagen synthesis, and epithelialization. Future research should focus on clinical trials to confirm the efficacy and safety of this treatment in human subjects. Additionally, exploring the use of SDF-1α/LLC in other types of chronic wounds could broaden its application and benefit a larger patient population.

Materials and methods

Study design

The objective of this study was to evaluate the efficacy of SDF-1α-loaded LLC hydrogel in promoting wound healing in both in vitro and in vivo models. The study used 40 male Wistar rats, divided into four groups of 10 rats each. A power analysis, assuming a large effect size (Cohen's $d = 0.8$) with a significance level of 0.05 and a desired power of 0.80, determined that 8–12 rats per group would be sufficient. Based on previous studies demonstrating significant differences in wound healing outcomes with similar treatments[27]a sample size of 10 rats per group was chosen. Data collection was conducted at pre-determined intervals (days 0, 3, 7, 14, and 21) without early stopping. Human dermal fibroblast cells were used for in vitro assays, and STZ-induced diabetic Wistar rats were used for in vivo experiments. The primary outcome measured was wound closure, with secondary outcomes including collagen deposition, epithelial thickness, and angiogenesis. Tukey's post hoc test was applied for multiple comparisons. Randomization was employed, and while the personnel applying treatments were not blinded, outcome assessors were blinded through coding, minimizing potential bias. Additionally, histological assessments were performed in a blinded manner, where the evaluator was unaware of the treatment group assignments. Tissue sections were coded before staining and analysis to ensure objective evaluation. Experiments were performed in triplicate to ensure reliability.

For in vitro experiments, each treatment condition was tested in at least six replicates per experimental set, following previous studies demonstrating statistical robustness with similar methodologies. All experiments were independently repeated three times to confirm reproducibility.

Materials

Phospholipid S100 (SPC, soy phosphatidylcholine) was supplied by Lipoid GmbH (Ludwigshafen, Germany). Glyceryl monooleate (GMO) was obtained from Dinfen Chemical Technology (Qingdao, China). Recombinant SDF-1α was sourced from SinoBiological, China. SDF-1/CXCL12 ELISA Kit was obtained from ZellBio, Germany and was used to measure SDF-1/CXCL12 levels in supernatant samples collected at specific time intervals during the release profile study. Streptozotocin was purchased from Dingyan Chem, China, and was used to induce Type 1 Diabetes Mellitus (T1DM) in male Wistar rats.

Preparation of LLC hydrogel formulations

The LLC hydrogel formulation was prepared by blending SPC and GMO in equal proportions (50:50 by weight). Ethanol was then added to the mixture at 10% of the total weight, serving as a co-solvent. The resulting mixture was subjected to bath sonication at 65 °C for 1.5 h at high power settings (70% amplitude) to ensure thorough mixing and homogenization of the components. After sonication, SDF-1α was added to the hydrogel under sterile conditions in a laminar flow hood, ensuring aseptic technique was maintained throughout the process, thus completing the formulation.

Characterization of formulations

Dynamic light scattering analysis of LLC hydrogel structure

To analyze the hydrogel structure using Dynamic Light Scattering (DLS), 100 µg of the LLC hydrogel was diluted with water to achieve an appropriate concentration for measurement. The dilution was performed to ensure the sample had an optimal particle concentration for DLS analysis. The sample was equilibrated at room temperature (approximately 25 °C) for 30 min to ensure consistent particle movement.

The diluted sample was then analyzed using the NanoBrook 90Plus DLS instrument (Brookhaven Instruments Corporation). The DLS measurements were conducted at a detection angle of 90 degrees. The instrument calculated the autocorrelation function of the intensity fluctuations, from which the size distribution of the particles within the hydrogel was determined. The hydrodynamic diameter of the particles, which provides insight into the hydrogel's structural characteristics, was reported. For accuracy, a standard latex particle size calibration sample was used to verify the instrument's performance prior to the analysis.

PLM analysis of LLC hydrogel

A portion of the LLC hydrogel was incubated in a sterile water-filled tube at room temperature for three days to facilitate the formation of the liquid crystalline phase. A thin layer of the hydrogel was then mounted between two glass slides, optimized for polarized light microscopy to preserve the structural integrity of hexosomes and cubosomes. The sample was examined using Polarized Light Microscopy (PLM) (BIOBASE BMP-107T, China). When illuminated with polarized light, the birefringent structures within the hydrogel split the light into two rays with different velocities, creating interference patterns upon passing through an analyzer. These patterns were analyzed to differentiate between hexagonal and cubic phases, with specific features such as brightness and shape under crossed polarizers indicating the presence of the liquid crystalline phases.

Rheological characterization

The liquid crystalline formulation samples were prepared and equilibrated at room temperature (25 °C) for 24 h prior to rheological analysis to ensure uniformity. The rheological properties of the samples were analyzed using a Brookfield R/S PLUS rheometer, equipped with C3-14 van spindles and Rheo3000 software. During the measurements, 3 ml of the equilibrated sample was loaded into a mini-slump apparatus (CC3-14). Viscosity measurements were conducted at a controlled temperature of 25 °C. The shear stress was linearly increased from 0 to 100 Pa. All measurements were performed in triplicate to ensure reproducibility. The data obtained from the Rheo3000 software were analyzed to assess key rheological parameters, including viscosity and shear-thinning behavior, providing insights into the flow characteristics of the formulation under varying shear conditions.

Water uptake/loss measurement

To study the water uptake/loss behavior, 100 µl of the LLC precursor was injected into 3 ml of PBS solution (pH 7.4) and incubated for 7 days. The water content was determined using Karl Fischer titration with a volumetric titrator (ARKA Sanat Arvin, Iran) at a controlled temperature of 25 °C. The Karl Fischer reagent, consisting of iodine, sulfur dioxide, and methanol, was freshly prepared and used in an airtight system to prevent moisture absorption. Samples were carefully weighed using a precision balance and then transferred to the titration vessel. Titration was initiated by continuously adding the Karl Fischer reagent from a burette while stirring the mixture at a constant rate. The titrator's detection system automatically identified the endpoint, halting reagent addition upon complete reaction of all water present with iodine. The water content percentage was calculated using the volume of Karl Fischer reagent consumed and the pre-determined titer value, following the formula:

$$\text{Water content } (\%) = \frac{\text{VKF} - \text{TKF}}{\text{W sample}} \times 100$$

Where:

$_{\text{KF}}$ = Volume of Karl Fischer reagent consumed.
$_{\text{KF}}$ = Titer of Karl Fischer reagent.
sample = Weight of the sample.

Degradation in vitro

Degradation pattern of the formulations was studied as described by Kamali et al.[39],. Briefly, each formulation was injected into vials containing PBS (150 mM, pH 7.4) using a 29-gauge needle and kept in a shaking incubator (37℃ 100 rpm). After the injection, the solution was turned to a hydrogel like phase. At predetermined time points (Days 1, 4, 7, 14, 21, 28, 42, 60), the resulting hydrogel was lyophilized and weighed.

SDF-1α release assay from LLC hydrogel

The release profile of SDF-1α from the LLC hydrogel was assessed in phosphate-buffered saline (PBS, pH 7.4) at 37 °C. A 100 mg sample of the hydrogel, containing 2000 ng of SDF-1α per gram, was placed in 1 mL of PBS in a centrifuge tube. The tube was placed on a rotator set to 30 rpm to ensure gentle mixing. At specific time intervals (1, 2, 4, 6, 24, 48, 72, and 144 h), 50 µL of PBS was removed and replaced with fresh PBS to maintain sink conditions. The collected samples were centrifuged at 10,000 g for 5 min, and the supernatant was analyzed using an ELISA method to quantify SDF-1α. To ensure stability, the pH of PBS was monitored before and after each time point, confirming a stable pH 7.4 ± 0.1 throughout the experiment. The release profile of SDF-1α was plotted over time, and data analysis, including the calculation of release kinetics, was performed using GraphPad Prism 8.4.3.

MTT-based cell viability assessment

The human dermal fibroblast cell line was cultured in DMEM with 10% FBS and 1% penicillin-streptomycin at 37 °C, 5% CO_2. At 80% confluency, cells were detached with trypsin-EDTA and seeded at 1×10^4 cells/well in 96-well plates. After 24 h adhesion, cells were treated for 24 h with varying concentrations of SDF-1 (6.25–800 ng/mL) and LLC (5, 10, and 15 µL); controls received medium only. MTT solution (20 µL, 5 mg/mL) was added and incubated for 4 h, then formazan was dissolved with 100 µL DMSO. Absorbance at 570 nm was measured. Cell viability (%) was normalized to controls. Experiments were performed in triplicate ($n = 3$). Data are mean ± SD. Statistical significance was evaluated by independent samples t-test ($p < 0.05$). IC_{50} was calculated using GraphPad Prism.

Scratch wound healing assay

A scratch wound healing assay was conducted using human dermal fibroblast (HDF) cells. The cells were cultured in DMEM supplemented with 10% fetal bovine serum and 1% penicillin-streptomycin at 37 °C in a 5% CO2 atmosphere until they reached confluence in 24-well plates. To inhibit cell proliferation and focus on cell migration, the cells were serum-starved for 24 h and treated with Mitomycin C (10 µg/mL) for 2 h prior to scratching. A sterile 200 µL pipette tip was used to create a scratch in the cell monolayer, which was then washed with PBS to remove detached cells. Wells were treated with various formulations, including allantoin (100 µg), LLC, SDF-1α 50 ng/LLC, SDF-1α 25 ng/LLC, SDF-1α 25 ng, and a negative control, with all treatments performed in triplicate.

Scratch closure was observed and imaged at 0, 12, and 24 h using an Olympus IX70 inverted phase microscope. The percentage of wound closure was calculated by comparing the initial wound area with subsequent wound areas. Data were analyzed using one-way ANOVA followed by Tukey's post hoc tests, with statistical significance set at $P < 0.05$.

In vivo study

Induction of type 1 diabetes mellitus

Forty male Wistar rats, sourced from animal house of Birjand University of Medical Sciences, were housed under controlled conditions (temperature 20–22 °C, humidity 60–70%, 12-hour light/dark cycle) with free access to standard laboratory chow and water. Type 1 diabetes mellitus was induced by intraperitoneal injection of 55 mg/kg streptozotocin (STZ) dissolved in citrate buffer (pH 4.5). To prevent hypoglycemia following STZ administration, a 10% sucrose solution was provided for 24 h, and the animals were monitored for any adverse reactions. Diabetes was confirmed 72 h later by fasting blood glucose levels above 200 mg/dL[40]. Only male Wistar rats aged 8–10 weeks, with a body weight range of 200–250 g, were included in the study. Rats with fasting blood glucose levels below 200 mg/dL after STZ injection were excluded from further analysis to ensure consistency in the diabetic model. Additionally, any rats showing signs of severe distress or weight loss exceeding 15% of initial body weight were humanely euthanized and excluded from the study.

Ethical statement

All experimental protocols involving animals were approved by the Institutional Animal Care and Use Committee (IACUC) of Birjand University of Medical Sciences, under protocol number IR.BUMS.REC.1401.001. All methods were carried out in accordance with relevant guidelines and regulations. The reporting of this study complies with the ARRIVE guidelines[41].

Euthanasia method

At the end of the experiment, rats were humanely euthanized by exposure to carbon dioxide (CO_2) in a controlled environment. The CO_2 concentration was gradually increased to ensure a humane and painless death in accordance with AVMA guidelines for the euthanasia of animals.

Experimental groups and wound creation

Animals were anesthetized with a combination of ketamine (70 mg/kg) and xylazine (6 mg/kg) administered intraperitoneally, as described in the wound healing protocol by Arunachalam et al. (2021)[42]. The rats were randomly divided into four groups to evaluate different treatments: a control group (no treatment), a group treated with plain LLC hydrogel, a group treated with LLC hydrogel containing 300 ng of SDF-1α, and a group treated with a PHMB gel containing polyhexamethylene biguanide and betaine (Treetta Tebasept Wound Gel X, Trita Company, Iran). Under anesthesia, full-thickness wounds (11 mm in diameter) were created on the dorsal region of each rat using a sterile biopsy punch, with two wounds per rat. Treatments were applied topically immediately after wound creation and were reapplied daily.

Wound healing was assessed by photographing the wounds on days 0, 3, 7, 14, and 21 post-injuries. Wound areas were measured using digital imaging software, and the percentage of wound closure was calculated. Data were analyzed using one-way ANOVA followed by Tukey's post hoc tests, with statistical significance set at $P < 0.05$.

Histopathological analysis

Tissue samples were fixed in 10% neutral buffered formalin for 24 h and subsequently embedded in paraffin. Sections 4–5 micrometers thick were cut using a Leitz 1512 Rotary Microtome (Leitz, Germany) and mounted on glass slides. The slides were stained with hematoxylin and eosin (H&E) for general histological assessment and with Masson's Trichrome for evaluating collagen deposition.

The stained slides were examined under a light microscope, and images from multiple fields were captured for analysis. Quantitative analysis of collagen deposition, epithelial thickness, angiogenesis, and counts of

fibroblastic and inflammatory cells was performed using ImageJ Fiji software. Statistical analysis was conducted using GraphPad Prism 8.4.3, employing ANOVA followed by Tukey's post hoc tests to determine significance, with a threshold of $P < 0.05$.

Statistics

Statistical analysis was performed using GraphPad Prism 8.4.3. Data were analyzed using one-way ANOVA followed by Tukey's post hoc tests to assess significance between groups. Before conducting ANOVA, Shapiro-Wilk tests were used to confirm normality of data distribution. In cases where normality assumptions were violated, Kruskal-Wallis tests were applied as a non-parametric alternative. Multiple comparisons were corrected using Tukey's post hoc test for parametric data and Dunn's test for non-parametric comparisons. Differences were considered statistically significant at $^{*}P < 0.05$, $^{**}P < 0.01$, $^{***}P < 0.001$, and ns for non-significant differences. Results are expressed as means ± SEM unless otherwise indicated. Each experiment was conducted in triplicate. All in vitro experiments were repeated two to four times to ensure reproducibility.

Data availability

The datasets used and/or analyzed during the current study are available from the corresponding author on reasonable request.

Received: 25 March 2025; Accepted: 7 July 2025
Published online: 18 July 2025

References

1. Kumar, A., Gangwar, R., Ahmad Zargar, A., Kumar, R. & Sharma, A. Prevalence of diabetes in india: A review of IDF diabetes atlas 10th edition. *Curr. Diabetes. Rev.* **20**, 105–114 (2024).
2. Nirenjen, S. et al. Exploring the contribution of pro-inflammatory cytokines to impaired wound healing in diabetes. *Front. Immunol.* **14**, 1216321 (2023).
3. Li, M., Hou, Q., Zhong, L., Zhao, Y. & Fu, X. Macrophage related chronic inflammation in non-healing wounds. *Front. Immunol.* **12**, 681710 (2021).
4. Jeffcoate, W. J., Vileikyte, L., Boyko, E. J., Armstrong, D. G. & Boulton, A. J. Current challenges and opportunities in the prevention and management of diabetic foot ulcers. *Diabetes Care*. **41**, 645–652 (2018).
5. Abedi, A. Recent approach for speeding up the wound healing. *J. Corona Virus*. **2**, 1–9 (2024).
6. Chen, J. et al. Neuropeptide substance P: a promising regulator of wound healing in diabetic foot ulcers. *Biochem. Pharmacol.* **215**, 115736 (2023).
7. Najar-Asl, M. et al. Transplantation of SDF-1α-loaded liver extracellular matrix repopulated with autologous cells attenuated liver fibrosis in a rat model. *EXCLI J.* **21**, 704 (2022).
8. Jiang, Q. et al. Modifying strategies for SDF-1/CXCR4 interaction during mesenchymal stem cell transplantation. *General Thorac. Cardiovasc. Surgery* **70**, 1–10 (2022).
9. Chatterjee, T. et al. Sex-Based disparities in leukocyte migration and activation in response to inhalation lung injury: role of SDF-1/CXCR4 signaling. *Cells* **12**, 1719 (2023).
10. Sadri, F., Rezaei, Z. & Fereidouni, M. The significance of the SDF-1/CXCR4 signaling pathway in the normal development. *Mol. Biol. Rep.* **49**, 3307–3320 (2022).
11. Groppa, E., Colliva, A., Vuerich, R., Kocijan, T. & Zacchigna, S. Immune cell therapies to improve regeneration and revascularization of non-healing wounds. *Int. J. Mol. Sci.* **21**, 5235 (2020).
12. Fang, J. et al. Stromal cell-derived factor-1 May play pivotal role in distraction-stimulated neovascularization of diabetic foot ulcer. *Med. Hypotheses*. **149**, 110548 (2021).
13. Yan, J. et al. Efficacy of topical and systemic transplantation of mesenchymal stem cells in a rat model of diabetic ischemic wounds. *Stem Cell Res. Ther.* **12**, 1–13 (2021).
14. Shafiq, M. et al. Combined effect of SDF-1 peptide and angiogenic cues in co-axial plga/gelatin fibers for cutaneous wound healing in diabetic rats. *Colloids Surf., B*. **223**, 113140 (2023).
15. Kim, B. S. et al. Myocardial ischemia induces SDF-1α release in cardiac surgery patients. *J. Cardiovasc. Transl. Res.* **9**, 230–238 (2016).
16. Malik, A. et al. Exogenous SDF-1α protects human myocardium from hypoxia-reoxygenation injury via CXCR4. *Cardiovasc. Drugs Ther.* **29**, 589–592 (2015).
17. Kaushik, K. & Das, A. Endothelial progenitor cell therapy for chronic wound tissue regeneration. *Cytotherapy* **21**, 1137–1150 (2019).
18. Olekson, M. A. P. et al. SDF-1 liposomes promote sustained cell proliferation in mouse diabetic wounds. *Wound Repair. Regeneration*. **23**, 711–723 (2015).
19. Guo, R. et al. Stromal cell-derived factor 1 (SDF-1) accelerated skin wound healing by promoting the migration and proliferation of epidermal stem cells. *Vitro Cell. Dev. Biology-Animal*. **51**, 578–585 (2015).
20. Chavda, V. P. et al. Lyotropic liquid crystals for parenteral drug delivery. *J. Controlled Release*. **349**, 533–549 (2022).
21. Arkas, M., Kitsou, I., Gkouma, A. & Papageorgiou, M. The role of hydrogen bonds in the mesomorphic behaviour of supramolecular assemblies organized in dendritic architectures. *Liquid Cryst. Reviews*. **7**, 60–105 (2019).
22. Silvestrini, A. V. P., Caron, A. L., Viegas, J., Praca, F. G. & Bentley, M. V. L. B. Advances in lyotropic liquid crystal systems for skin drug delivery. *Expert Opin. Drug Deliv.* **17**, 1781–1805 (2020).
23. Das, S., Bora, U. & Borthakur, B. in *Silk Biomaterials for Tissue Engineering and Regenerative Medicine* 41–77Elsevier, (2014).
24. Usui, M. L., Mansbridge, J. N., Carter, W. G., Fujita, M. & Olerud, J. E. Keratinocyte migration, proliferation, and differentiation in chronic ulcers from patients with diabetes and normal wounds. *J. Histochem. Cytochemistry*. **56**, 687–696 (2008).
25. Sharma, P., Dhawan, S. & Nanda, S. Cubosome: a potential liquid crystalline carrier system. *Curr. Pharm. Design*. **26**, 3300–3316 (2020).
26. Karimi, M. et al. Prolonged local delivery of doxorubicin to cancer cells using lipid liquid crystalline system. *Int. J. Pharm.* **639**, 122947 (2023).
27. Zhu, Y. et al. Sustained release of stromal cell derived factor-1 from an antioxidant thermoresponsive hydrogel enhances dermal wound healing in diabetes. *J. Controlled Release*. **238**, 114–122 (2016).
28. Xiao, L. et al. Overexpression of TGF-β1 and SDF-1 in cervical cancer-associated fibroblasts promotes cell growth, invasion and migration. *Arch. Gynecol. Obstet.* **305**, 179–192 (2022).
29. Yao, C. H., Chen, K. Y., Cheng, M. H., Chen, Y. S. & Huang, C. H. Effect of Genipin crosslinked Chitosan scaffolds containing SDF-1 on wound healing in a rat model. *Mater. Sci. Engineering: C.* **109**, 110368 (2020).

30. Li, Q., Guo, Y., Chen, F., Liu, J. & Jin, P. Stromal cell-derived factor-1 promotes human adipose tissue-derived stem cell survival and chronic wound healing. *Experimental Therapeutic Med.* **12**, 45–50 (2016).
31. Rabbany, S. Y. et al. Continuous delivery of stromal cell-derived factor-1 from alginate scaffolds accelerates wound healing. *Cell Transplant.* **19**, 399–408 (2010).
32. Ceradini, D. J. et al. Progenitor cell trafficking is regulated by hypoxic gradients through HIF-1 induction of SDF-1. *Nat. Med.* **10**, 858–864 (2004).
33. Rajabalaya, R., Musa, M. N., Kifli, N. & David, S. R. Oral and transdermal drug delivery systems: role of lipid-based lyotropic liquid crystals. *Drug Des. Dev. Therapy* **11**, 393–406 (2017).
34. El Kheir, W. et al. Impact of simulated brain interstitial fluid flow on the chemokine CXCL12 release from an alginate-based hydrogel in a new 3D in vitro model. *Front. Drug Delivery*. **3**, 1227776 (2023).
35. Tang, G. et al. Recent advances of chitosan-based injectable hydrogels for bone and dental tissue regeneration. *Front. Bioeng. Biotechnol.* **8**, 587658 (2020).
36. Li, L. et al. SDF-1α/OPF/BP Composites Enhance the Migrating and Osteogenic Abilities of Mesenchymal Stem Cells. *Stem Cells International* 1938819 (2021). (2021).
37. Jarrah, A. A. et al. SDF-1 induces TNF-mediated apoptosis in cardiac myocytes. *Apoptosis* **23**, 79–91 (2018).
38. Maan, Z. N., Borrelli, M. R., Houschyar, K. S. & Gurtner, G. C. Stromal cell-derived factor 1 (SDF-1) signaling and tissue homeostasis. *Regenerative medicine and plastic surgery: elements, Research concepts and Emerging technologies*, 47–59 (2019).
39. Khodaverdi, E. et al. In-vitro and in-vivo evaluation of sustained-release buprenorphine using in-situ forming lipid-liquid crystal gels. *Life Sci.* **314**, 121324 (2023).
40. Wickramasinghe, A. S. D., Attanayake, A. P. & Kalansuriya, P. Biochemical characterization of high fat diet fed and low dose streptozotocin induced diabetic Wistar rat model. *J. Pharmacol. Toxicol. Methods*. **113**, 107144 (2022).
41. Kilkenny, C., Browne, W. J., Cuthill, I. C., Emerson, M. & Altman, D. G. Improving bioscience research reporting: the ARRIVE guidelines for reporting animal research. *PLoS Biol.* **8** https://doi.org/10.1371/journal.pbio.1000412 (2010).
42. Arunachalam, K., Sasidharan, S. P., Arunachalam, K. & Sasidharan, S. P. Animal experiment of wound healing activity. *Bioassays Experimental Preclinical Pharmacology*, 105–118 (2021).

Author contributions

F.S., H.S., and M.F. conceptualized the study. H.S., H.K., and M.F. designed the methodology. F.S., Z.R., H.S., H.K., M.S., P.M.-T., and M.F. conducted the investigation. F.S., Z.R., and H.K. contributed to data visualization. M.F. administered the project. M.F. and H.S. supervised the study. F.S., H.S., and M.F. drafted the original manuscript. H.S., H.K., and M.F. reviewed and edited the final manuscript. All authors read and approved the final version of the manuscript.

Declarations

Competing interests

The authors declare no competing interests.

Additional information

Correspondence and requests for materials should be addressed to M.F.

Reprints and permissions information is available at www.nature.com/reprints.

Publisher's note Springer Nature remains neutral with regard to jurisdictional claims in published maps and institutional affiliations.